Isovector stretched-state excitations in the ^{20}Ne, ^{24}Mg, ^{28}Si, and ^{32}S(p,n) reactions at 136 MeV

N. Tamimi, B. D. Anderson, A. R. Baldwin, T. Chittrakarn, M. Elaasar, R. Madey, D. M. Manley, M. Mostajabodda'vati, J. W. Watson, and W.-M. Zhang
Department of Physics, Kent State University, Kent, Ohio 44242

J. A. Carr
Supercomputer Computations Research Institute, The Florida State University, Tallahassee, Florida 32306

C. C. Foster
Indiana University Cyclotron Facility, Bloomington, Indiana 47408
(Received 17 September 1991)

Isovector stretched-state excitations were studied in the (p,n) reaction at 136 MeV on the self-conjugate *s-d* shell nuclei ^{20}Ne, ^{24}Mg, ^{28}Si, and ^{32}S. The measurements were performed in three separate experiments using the beam-swinger neutron time-of-flight facility at the Indiana University Cyclotron Facility. Neutrons were detected in large-volume plastic scintillation detectors located in three detector stations at 0°, 24°, and 45° with respect to the undeflected beam line; the flight paths varied from 75 to 134 m. Overall time resolutions of about 825 ps provided energy resolutions of about 320 keV in the first two stations and about 425 keV in the third station. Both $(d_{5/2},d_{5/2}^{-1})5^+$ $0\hbar\omega$ and $(f_{7/2},d_{5/2}^{-1})6^-$ $1\hbar\omega$ stretched-state excitations are observed in the (p,n) reaction on ^{20}Ne, ^{24}Mg, and ^{28}Si. For the (p,n) reaction on ^{32}S, only the 6^- strength is observed. The states are identified by comparison of the extracted angular distributions with distorted-wave impulse-approximation calculations and by comparison with known analog states observed in inelastic scattering. In the ^{20}Ne and ^{24}Mg(p,n) reactions, the majority of the 5^+ strength is observed in single states at low excitation energy; the strengths are described well by full *s-d* shell-model calculations. A weak 5^+ state is observed in the ^{28}Si$(p,n)^{28}$P reaction that corresponds to the strength expected if there is $\sim\frac{1}{3}$ of a hole in the $d_{5/2}$ proton orbital. The 6^- $1\hbar\omega$ strength is fragmented in all four reactions. Less than 60% of the strength expected in the extreme single-particle-hole model is observed in each case. The observed 6^- strengths and distributions in the ^{28}Si and ^{32}S(p,n) reactions are described well by large-basis shell-model calculations.

PACS number(s): 25.40.Hs, 27.30.+t

I. INTRODUCTION

This paper reports the study of particle-hole stretched-state excitations with the (p,n) reaction at 136 MeV on the *s-d* shell, self-conjugate nuclei ^{20}Ne, ^{24}Mg, ^{28}Si, and ^{32}S. Particle-hole stretched-state excitations, formed by a pair involving the highest-spin orbitals in their respective shells coupled to the maximum angular momentum, are expected to be relatively pure shell-model states. These particle-hole couplings are unique within $2\hbar\omega$ of excitation, and only more complicated configurations can mix with these states. Comparison with structure calculations of the measured strength and fragmentation of these stretched states provides an important test of such calculations.

Stretched-state excitations have been studied with a variety of reactions, including proton and electron inelastic scattering [1], particle-transfer reactions [2], and charge-exchange reactions [3]. These various reactions provide both supplementary and complementary information regarding stretched-state excitations; accordingly, one should consider all of this information simultaneously in order to obtain the fullest understanding. The (p,n) charge-exchange reaction provides important contributions to this systematic approach. Because the (p,n) reaction is strictly isovector, the absence of isoscalar strength allows unambiguous identification of the isovector strength. For the case of self-conjugate target nuclei, the (p,n) reaction will excite only the $T=1$ strength. Comparison of the (p,n) results with inelastic-scattering [e.g., (p,p') or (e,e')] excitation of the analog states in the target nucleus permits the $T=0$ and 1 states to be identified uniquely. Earlier examples that use the (p,n) reaction to take advantage of the isovector selectivity include studies of stretched-state excitations on the self-conjugate targets ^{16}O and ^{40}Ca [4,5]. In the case of ^{40}Ca(p,n), the suppression of the isoscalar background allowed the identification of highly fragmented $(f_{7/2},d_{5/2}^{-1}),6^-$ stretched-state strength. This strength had been looked for in (e,e') and (p,p') studies but could not be identified because of the fragmentation and strong isoscalar ($T=0$) background.

In this work, we extend the earlier (p,n) studies to the *s-d* shell, self-conjugate nuclei ^{20}Ne, ^{24}Mg, ^{28}Si, and ^{32}S. Stretched-state excitations in these nuclei have been, or are being, studied via inelastic electron or proton scattering. In addition, the (p,n) excitation of the strongest 6^- stretched-state excitation in the ^{28}Si$(p,n)^{28}$P reaction was reported earlier [6].

The $(f_{7/2},d_{5/2}^{-1}),6^-$ stretched-state excitations in ^{24}Mg

and ^{28}Si were among the first particle-hole stretched-state excitations to be studied. The strongest states in both cases have been observed in both inelastic proton and electron scattering [7–9]. The emphasis in these earlier studies, as well as the earlier (p,n) work on ^{28}Si, was to compare the observed strength of the most strongly excited state with the simple shell-model predictions. These strength comparisons are based on using impulse-approximation calculations, assuming the dominance of single-step mechanisms [viz., the distorted-wave impulse approximation (DWIA)]. In all cases, less than one-half of the simple shell-model strength was observed. It is now recognized that most of this reduction in observed strength is due to configuration mixing of the nuclear states. Amusa and Lawson [10] showed that a large-basis shell-model calculation could explain at least one-half of the reduction observed for the $T=1$, $(f_{7/2},d_{5/2}^{-1}),6^-$ state in the $A=28$ system. More recently, Carr *et al.* [11] performed an even larger-basis calculation, which appears to describe the observed strength in the strongest state reasonably well. If this explanation is correct, then one would expect to see some of the stretched-state strength removed by configuration mixing with other states. In particular, Carr *et al.* [11] showed a predicted spectrum for ^{28}Si with a cluster of strength about 3 MeV above the strongest $T=1$ state; however, identification is difficult because of isoscalar backgrounds in inelastic-scattering studies. The (p,n) reaction provides the suppression of this background and is the reaction best suited to study the fragmentation of the isovector stretched-state strength. The comparison of the observed fragmentation with the large-basis, shell-model calculations will provide a different level of test of the completeness of this fragmentation as the explanation of the reduction of stretched-state strength.

In addition to the excitation of "$1\hbar\omega$" stretched states, the (p,n) charge-exchange reaction can excite also "$0\hbar\omega$" stretched states in nuclei. These states involve creating a particle-hole pair (1p-1h) in the same major shell. If the particle and hole are both in the largest-j orbital in the shell, and couple to the maximum possible angular momentum, then the state is the maximum stretched state in that shell. Similar to $1\hbar\omega$ stretched states, these states are unique $1p$-$1h$ states within $2\hbar\omega$ of excitation. Because these states involve creating a proton-particle, neutron-hole state in the same orbital, they can be formed only in charge-exchange reactions. Indeed, such "$0\hbar\omega$" stretched states have been observed in many nuclei with the (p,n) reaction above 100 MeV [12]. Because these $0\hbar\omega$ excitations usually involve orbitals near the Fermi surface, they are typically less fragmented than are $1\hbar\omega$ stretched states; the DWIA normalization factors for $0\hbar\omega$ stretched states are typically twice as large as they are for $1\hbar\omega$ stretched states.

In this work, we expect to see $(d_{5/2},d_{5/2}^{-1}),5^+$ $0\hbar\omega$ stretched-state excitations in the (p,n) reaction on ^{20}Ne and ^{24}Mg. For ^{28}Si and ^{32}S, in the simple shell model, the $d_{5/2}$ orbital is full for protons (and neutrons) so that the state is blocked; any 5^+ strength observed would be a direct indication of ground-state correlations. Because these states involve the valence orbitals, they are expected at low excitation energies in the residual nuclei, well below the 6^- $1\hbar\omega$ excitations.

In fact, fragmented 6^- "$1\hbar\omega$" stretched-state strength is observed in all four reactions, and 5^+ "$0\hbar\omega$" strength is observed in the (p,n) reaction on ^{20}Ne, ^{24}Mg, and ^{28}Si. These results are described below and compared with the earlier inelastic-scattering results and with DWIA calculations using realistic shell-model wave functions. Angular distributions corresponding to 4^- excitations are observed also; however, these can be a mixture of both $(d_{5/2},p_{3/2}^{-1})$ and $(f_{7/2},d_{5/2}^{-1})$ 1p-1h configurations, so that they are not unique like the 5^+ and 6^- excitations (in the simple shell model). For more detail see Ref. [13].

II. EXPERIMENTAL PROCEDURE

The measurements were performed at the Indiana University Cyclotron Facility with the beam-swinger system. The experimental arrangement and data-reduction procedures were similar to those described previously [14]. Neutron kinetic energies were measured by the time-of-flight (TOF) technique. A beam of 136-MeV protons was obtained from the cyclotron in narrow beam bursts typically 350 ps long, separated by 132.7 ns. Neutrons were detected in three detector stations at 0°, 24°, and 45° with respect to the undeflected proton beam. For the ^{20}Ne and ^{24}Mg measurements, the flight paths were 131.0, 131.1, and 81.4 m, respectively. For the ^{28}Si(p,n) measurements, the corresponding flight paths were 90.9, 90.8, and 74.4 m. For the ^{32}S(p,n) measurements, the flight paths were 125.2, 133.6, and 80.9 m, respectively. The neutron detectors were rectangular bars of fast plastic scintillator 10.2 cm thick. Three separate detectors each 1.02 m long by 0.51 m high were combined for a total frontal area of 1.55 m^2 in the 0° and 24° stations. Two detectors were used in the 45° station; both were 1.52 m long by 0.76 m high, for a combined frontal area of 2.31 m^2. Each neutron detector had tapered plexiglass light pipes attached on the two ends coupled to 12.8-cm-diam phototubes. Timing signals were derived from each end and combined in a mean-timer circuit to provide the timing signal from each detector. Overall time resolutions of about 820 ps were obtained, including contributions from the beam burst width ($\sim$350 ps) and energy spread ($\sim$480 ps), energy loss in the target ($\sim$300 ps), neutron transit times across the 10.2-cm thickness of the detectors ($\sim$550 ps), and the intrinsic time dispersion of each detector ($\sim$300 ps). This overall time resolution provided an energy resolution of about 320 keV in the first two detector stations and about 480 keV in the widest-angle station. The large-volume neutron detectors were described in more detail previously [15]. Protons from the target were rejected by anticoincidence detectors in front of each neutron detector array. Cosmic rays were vetoed by anticoincidence detectors on top as well as the ones at the front of each array.

The ^{24}Mg and ^{28}Si targets were self-supporting foils 29.2 ± 1.5 and 42.1 ± 0.9 mg/cm^2 thick, respectively. The ^{20}Ne target was a 4-cm-long gas cell with 0.5-mil Kapton windows filled to $\sim$3 atm. (absolute). (Empty cell "background" runs were performed to subtract the window

contributions from the TOF spectra.) The ^{32}S target was a 43.8-mg/cm^2 self-supporting foil of Li_2S, which was made by pressing Li_2S powder in a steel die. The $^{32}S(p,n)$ spectra were obtained by subtraction of TOF spectra obtained from a 40.8-mg/cm^2 Li-foil target. This subtraction and the $^{32}S(p,n)$ experiment are described in more detail in Ref. [16]. Time-of-flight spectra were obtained at $\sim$15 angles between 0° and 63°. Spectra from each detector were recorded at many pulse-height thresholds ranging from 25 to 90 MeV equivalent-electron energy (MeVee). Calibration of the pulse-height response of each of the detectors was performed with a ^{228}Th gamma source, which emits a 2.61-MeV gamma ray, and a calibrated fast amplifier. The values of the cross sections extracted for several thresholds (from 40 to 70 MeVee) were found to be the same within statistics.

III. DATA REDUCTION

Excitation-energy spectra were obtained from the measured TOF spectra using the known flight path and a calibration of the time-to-amplitude converter. Known states in the residual nuclei provided absolute reference points. Absolute neutron kinetic energies (and therefore excitation energies) are believed to be accurate to ± 0.1 MeV.

Yields for individual transitions were obtained by peak fitting of the TOF spectra. The spectra were fitted with an improved version of the peak-fitting code of Bevington [17]. Examples of the peak fitting at 45° (where the stretched-state excitations dominate) are shown in Fig. 1.

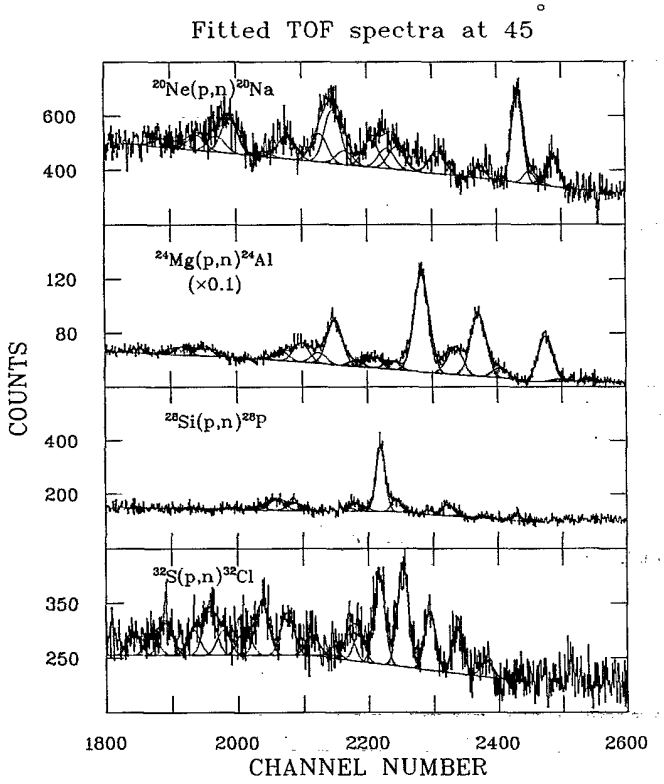

FIG. 1. Fits to the time-of-flight spectra at 45° for the ^{20}Ne, ^{24}Mg, ^{28}Si, and $^{32}S(p,n)$ reactions at 136 MeV.

The TOF spectra were subdivided into regions where groups of peaks and a smooth polynomial background could be fitted simultaneously. The minimum number of peaks required to fit the data was used, consistent also with the requirement that the fits proceed reasonably from one angle to the next. Widths for small peaks were constrained to be the same as those observed for the largest peak in each group. Cross sections were obtained by combining the yields with the measured geometrical parameters, the beam integration, and the target thickness. The neutron detector efficiencies were obtained from a Monte Carlo computer code [18], which was tested extensively at these energies [19,20]. The experimental procedure and data reduction is similar to that described in more detail in Ref. [14]. The uncertainty in the overall scale factor is dominated by the uncertainty in the detector efficiencies and is estimated to be $\pm 12\%$. The uncertainty estimated for each transition was taken as the quadratic sum of this scale uncertainty, plus $\pm 10\%$ as a minimum uncertainty in the fitting process, plus ± 0.008 mb/sr as an absolute minimum uncertainty in extracted cross sections. (The latter was estimated as $\sim \pm 50\%$ of the smallest cross sections extracted.)

IV. RESULTS

Both 5^+ $0\hbar\omega$ and 6^- $1\hbar\omega$ stretched-state strength is observed in the (p,n) reaction on ^{20}Ne, ^{24}Mg, and ^{28}Si. For the (p,n) reaction on ^{32}S, 5^+ strength is not observed. These results are presented individually below.

The various J^π assignments were made based on the analysis of extracted angular distributions and comparisons with known analog states. The angular distributions are compared with distorted-wave impulse-approximation (DWIA) calculations in order to establish l transfers and to obtain spectroscopic strength. These calculations were performed with the code DWBA70 [21]; the nucleon-nucleon effective interaction assumed is that of Franey and Love at 140 MeV [22]. The optical-model parameters used were those of Olmer *et al.*, obtained for proton elastic scattering on ^{28}Si [8]. The structure assumed was just the simple shell model; i.e., the 0^+ target wave functions are those expected in the simple shell model and the final states were assumed to be either $(\pi d_{5/2}, \nu d_{5/2}^{-1}), 5^+$ or $(\pi f_{7/2}, \nu d_{5/2}^{-1}), 6^-$ one-particle–one-hole states excited from the ground-state configurations. We refer to this as the extreme single-particle-hole model (ESPHM). The normalization factors required to make the DWIA calculations agree in magnitude with the experimental angular distributions we label as S^2. For each case then, the value expected in the ESPHM is $S^2=1$. The DWIA normalization factors quoted all include the correction factor $[(A-1)/A]^{\Delta J-1}$, to account for center-of-mass motion [23].

The harmonic-oscillator parameters for the DWIA calculations were taken from the A-dependent formula of Blomquist and Molinari [24] and adjusted slightly ($\leq 7\%$) to provide the best overall fits to the strongest 5^+ and 6^- angular distributions for each target. The resulting values were found to be $b=1.70$, 1.82, 1.74, and 1.77 fm^{-1}, for ^{20}Ne, ^{24}Mg, ^{28}Si, and ^{32}S, respectively. The values for ^{24}Mg, ^{28}Si, and ^{32}S are within 2% of the values

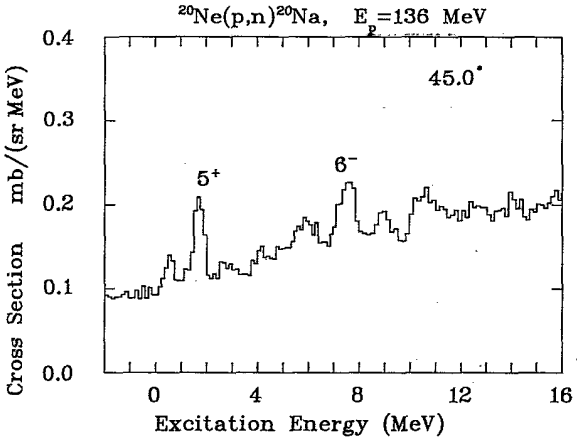

FIG. 2. Excitation-energy spectrum for the ^{20}Ne$(p,n)^{20}$Na reaction at 136 MeV and 45°.

found in inelastic-electron-scattering analyses of high-spin state excitations in these nuclei (no electron-scattering analysis is available for ^{20}Ne) [1,25].

A. The ^{20}Ne$(p,n)^{20}$Na reaction

The experimental excitation-energy plot for this reaction at 45.0° is shown in Fig. 2. The dominant 5^+ and 6^- peaks are labeled.

The strong excitation observed at 1.9 MeV is in good agreement with the known 5^+ state at 1.82 MeV in ^{20}F, the analog, $T=1$ nucleus [26]. The analog state is part of a complex of five states, between 1.82 and 2.19 MeV in ^{20}F, which, if present also in ^{20}Na, could not be resolved in this experiment. These states include a 2^-, a 3^-, a 2^+, and a 3^+ state, besides the 5^+ state. The extracted angu-

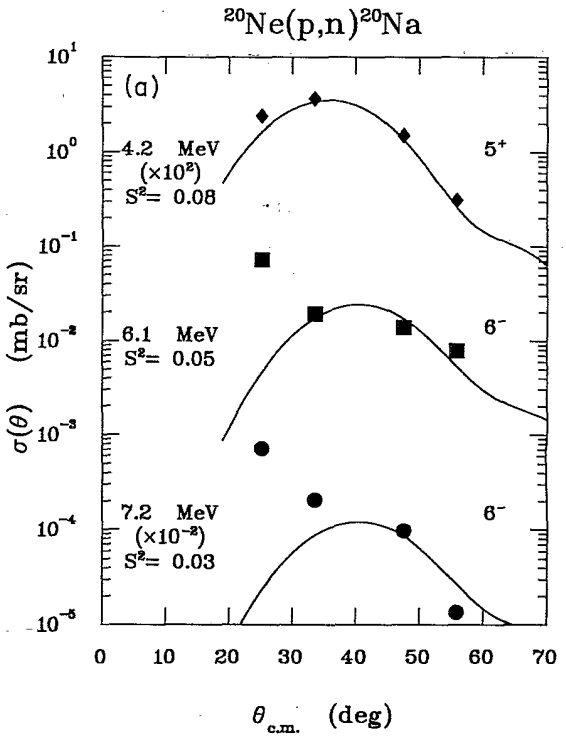

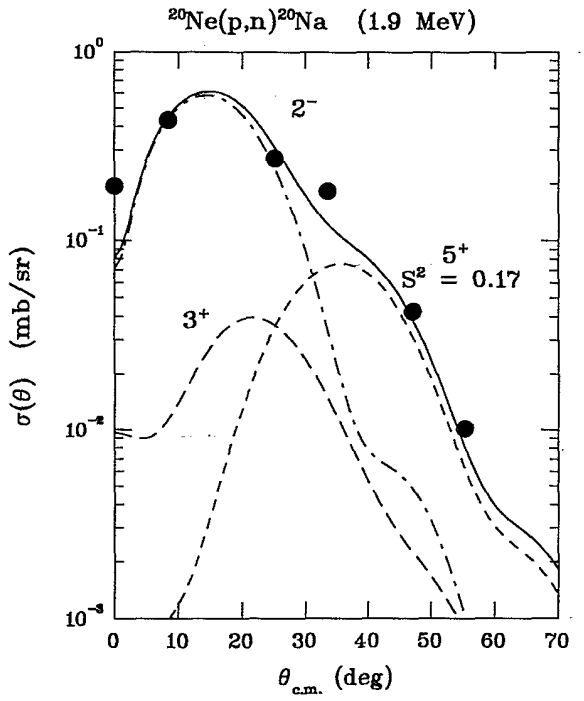

FIG. 3. Angular distribution for the 2^-, 3^+, and 5^+ complex at 1.9 MeV in the ^{20}Ne$(p,n)^{20}$Na reaction at 136 MeV. The lines represent DWIA calculations (see the text).

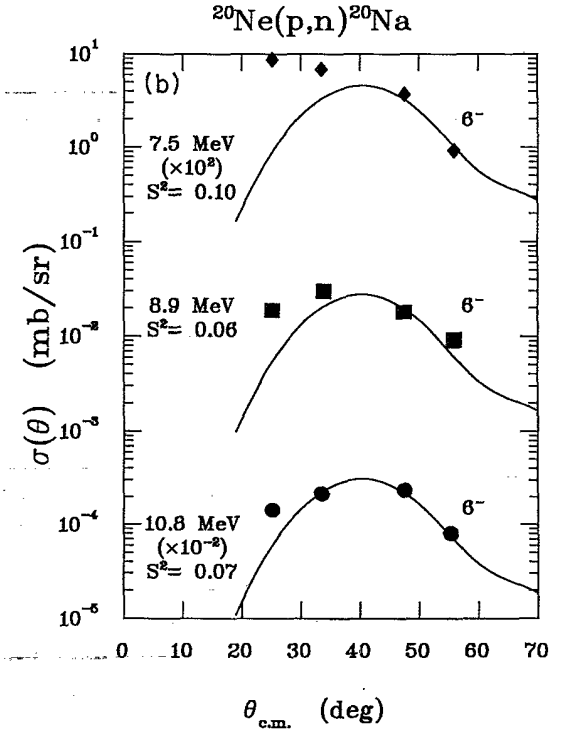

FIG. 4. Angular distributions for the 5^+ state at 4.2 MeV and the 6^- states at 6.1, 7.2, 7.5, 8.9, and 10.8 MeV. The solid lines represent DWIA calculations (see the text).

lar distribution for this complex, shown in Fig. 3, is fitted well by a combination of DWIA calculations for 2^-, 3^+, and 5^+ transitions. The wave functions for the 3^+ and 5^+ states (and for the ^{20}Ne target nucleus) were obtained from a full *s-d* shell-model calculation performed using the code OXBASH [27] with the "universal *s-d*" interaction of Wildenthal [28]. Consistent with the known (analog) states in ^{20}F, the wave function assumed for the 3^+ state is that calculated for the second 3^+ state. The wave function for the 2^- state was calculated using a model space including up to 5p-5h configurations from the simple shell model for ^{20}Ne in the $(d_{5/2},p_{3/2},p_{1/2})$orbitals. The interaction assumed was the Millener-Kurath *psd* interaction [29]. The 2^+ and 3^- contributions were calculated to be relatively small and were not needed to obtain a good fit to the angular distribution. In any event, the 5^+ contribution is seen to dominate the angular distribution cross section at wide angles; it is 80–90 % of the total cross section at angles beyond 40°. None of the contributions from the other unresolved states can affect significantly the required normalization for the 5^+ state. As shown, the required 5^+ DWIA normalization factor is $S^2=0.17$ if one assumes only the extreme single-particle-hole model (ESPHM) for the structure of the 5^+ state, built on the simple shell model for ^{20}Ne [viz., $(\pi d_{5/2}^2,\nu d_{5/2}^2)$ for the 0^+ g.s. and $(d_{5/2},d_{5/2}^{-1})$ for the 5^+ final state].

In addition to the 5^+ state at 1.9 MeV, a small peak is observed at 4.2 MeV which has a wide-angle angular distribution that is consistent with a weak 5^+ state; the angular distribution is not fit well by either a 4^- or 6^- DWIA calculation (see Fig. 4). The strength of this state is less than one-half of the strong 5^+ state at 1.9 MeV.

At least five states are observed which appear to be 6^- $1\hbar\omega$ excitations in the ^{20}Ne$(p,n)^{20}$Na reaction. These states are seen in Fig. 2 at 6.1, 7.2, 7.5, 8.9, and 10.8 MeV. The angular distributions for these five transitions are shown in Fig. 4. The DWIA calculations shown assume the simple shell model so that the 6^- state is taken to be pure $(f_{7/2},d_{5/2}^{-1})$. As shown, the wide-angle portions of the angular distributions are fit well by a 6^- DWIA calculation. No DWIA calculation for another J^π will fit as well; the 6^- strength in these states appears unambiguous. Based on the DWIA normalizations shown in Fig. 4, the total 6^- strength observed is (32±5)% of that expected in the ESPHM. In addition to the 5^+ and 6^- strengths, 4^- strength is observed in transitions to states at 6.5 and 7.8 MeV.

The stretched-state strength observed in the ^{20}Ne$(p,n)^{20}$Na reaction is summarized in Table I.

B. The ^{24}Mg$(p,n)^{24}$Al reaction

The experimental excitation-energy plot for this reaction at 45° is shown in Fig. 5. The dominant 5^+ and 6^- peaks are indicated.

The strong excitation observed at 1.6 MeV is in good agreement with the known 5^+ state at 1.5 MeV in ^{24}Na, the analog $T=1$ nucleus [26]. The analog state is part of a complex of four states between 1.3 and 1.5 MeV in ^{24}Na, which, if present also in ^{24}Al could not be resolved in this experiment. These states include a 1^+, a 2^+, and a 3^+ state, besides the 5^+ state. The (p,n) angular distribution for this complex is shown in Fig. 6. The angular

TABLE I. Excitation energies and spectroscopic strengths for stretched-state excitations observed in this work. The strengths (S^2) are expressed as a fraction of that expected in the extreme single-particle-hole model S^2 (ESPHM). The fraction of extreme single-particle-hole model (ESPHM), is given by $S^2=N_{\rm DWIA}[(A-1)/A]^{\Delta J-1}$, see the text, Sec. IV. Parentheses indicate estimated uncertainties, see the text, Sec. III. S^2 (ESPHM)$=Z^2$, the square of the one-body transition density in the simple shell model.

^{20}Ne$(p,n)^{20}$Na		^{24}Mg$(p,n)^{24}$Al		^{28}Si$(p,n)^{28}$P		^{32}S$(p,n)^{12}$Cl	
E_x (MeV)	S^2	E_x (MeV)	S^2	E_x (MeV)	S^2	E_x (MeV)	S^2
			5^+				
1.9	0.171(0.028)	1.6	0.300(0.048)	2.5	0.042(0.010)		
4.2	0.081(0.015)	4.7	0.180(0.029)	4.7	0.014(0.008)		
$\sum S^2$ (exp)	0.252(0.040)		0.480(0.076)		0.056(0.012)		
$\sum S^2$ (the)	0.096		0.122		0.094		
S^2 (ESPHM)	0.222		0.222		0.000		
			6^-				
6.1	0.054(0.012)	3.9	0.144(0.024)	5.0	0.250(0.040)	3.8	0.068(0.013)
7.2	0.031(0.009)	5.5	0.242(0.039)	5.9	0.013(0.008)	4.7	0.077(0.014)
7.5	0.103(0.018)	8.2	0.105(0.018)	7.8	0.033(0.010)	5.6	0.119(0.020)
8.9	0.062(0.013)	8.5	0.023(0.009)	8.4	0.050(0.011)	6.3	0.102(0.018)
10.8	0.070(0.014)	8.7	0.023(0.009)	8.9	0.033(0.010)	6.8	0.034(0.010)
		9.2	0.057(0.024)	9.2	0.019(0.009)	7.4	0.047(0.011)
		9.7	0.028(0.012)	10.1	0.019(0.009)	8.4	0.013(0.008)
				11.2	0.012(0.008)	9.2	0.038(0.010)
						9.8	0.051(0.011)
$\sum S^2$ (exp)	0.320(0.051)		0.622(0.098)		0.429(0.068)		0.549(0.086)
$\sum S^2$ (the)	0.604		0.747		0.771		0.903
S^2 (ESPHM)	0.333		0.667		1.000		1.000

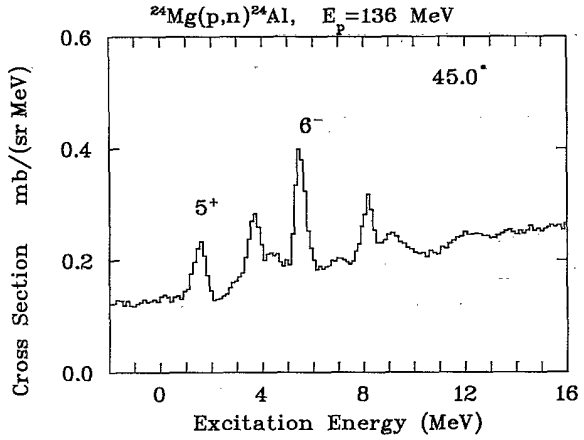

FIG. 5. Excitation-energy spectrum for the ^{24}Mg$(p,n)^{24}$Al reaction at 136 MeV and 45°.

distribution is fit well by a combination of DWIA calculations for 1^+, 2^+, 3^+ and 5^+ transitions. The wave functions were obtained from a full *s-d* shell-model calculation performed using the code OXBASH [27]. As for the positive-parity excitations in ^{20}Na, the interaction assumed is the universal *s-d* interaction of Wildenthal [28]. The 5^+ contribution dominates the angular distribution at angles greater than 40°. The DWIA normalization factor (S^2) required for the 5^+ contribution is 0.30, if one assumes only the ESPHM. In addition to this strong excitation, there is evidence for additional 5^+ strength at 4.7 MeV. The angular distribution for the latter is clearly dominated by a high multi-polarity excitation. The wide-angle portion is fit well by a DWIA calculation for a 5^+ excitation ($\Delta l=4$). No other high-spin transition will fit as well (viz., 4^- or 6^-). The DWIA normalization factor for this transition in the ESPHM is $S^2=0.18$. The summary of the 5^+ strength observed in the ^{24}Mg$(p,n)^{24}$Al reaction is presented in Table I.

At least seven states are observed in the ^{24}Mg$(p,n)^{24}$Al reaction that appear to be 6^- $1\hbar\omega$ excitations. These states are seen in Fig. 5 at 3.9, 5.5, 8.2, 8.5, 8.7, 9.2, and 9.7 MeV. The largest excitation is to the state at 5.5 MeV. The analog of this 6^- state is seen also in inelastic electron and proton scattering, at $E_x=15.1$ MeV in ^{24}Mg [7,9]. In Fig. 7, the (p,n) cross-section angular distribution for this transition is presented together with twice the (p,p') angular distribution measured by Adams *et al.* [7]. (The factor of 2 is just the ratio of the isospin geometrical factors.) The two experimental angular distributions are in good agreement and are fit well by a DWIA calculation for a transition to a $(f_{7/2},d_{5/2}^{-1}),6^-$ particle-hole state. (The disagreement at forward angles is due to contributions to the experimental angular distribution from unresolved states of lower spin.) The DWIA normalization factor, assuming the ESPHM, is 0.24.

The angular distributions for the other six transitions that appear to have 6^- strength are compared with DWIA calculations in Fig. 8. In general, the wide-angle parts of these distributions are fit well by the 6^- calculations and the assignments appear reliable. The worst case

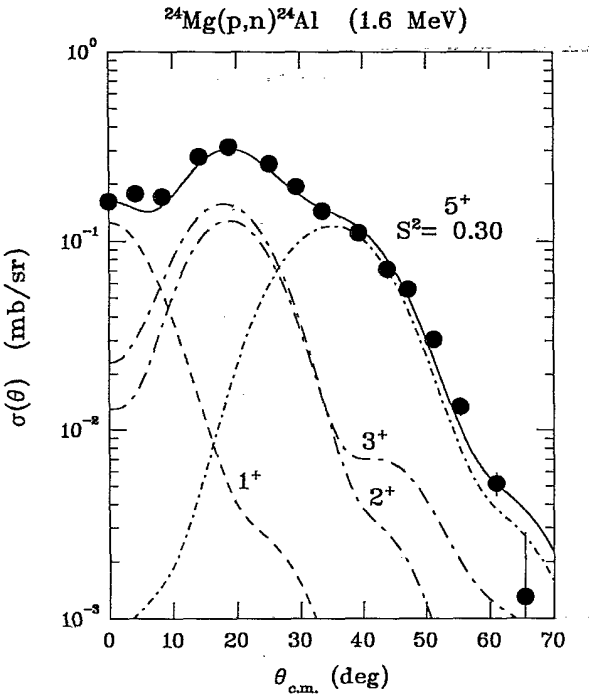

FIG. 6. Angular distribution for the 1^+, 2^+, 3^+, and 5^+ state complex at 1.6 MeV in the ^{24}Mg$(p,n)^{24}$Al reaction at 136 MeV. The lines represent DWIA calculations (see the text).

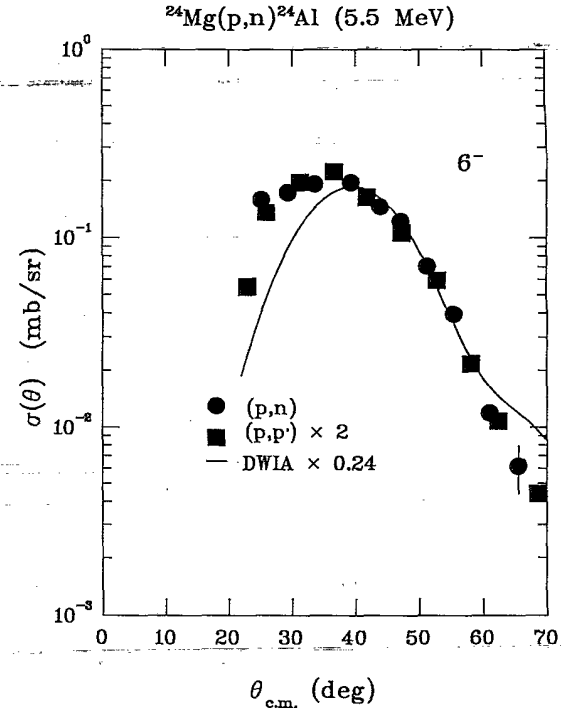

FIG. 7. Angular distribution for the 6^- excitation at 5.5 MeV in the ^{24}Mg$(p,n)^{24}$Al reaction at 136 MeV. Shown also are the (p,p') measurements to the analog 6^- state in ^{24}Mg (Ref. [9]). The solid line represents a DWIA calculation (see the text).

is for the 3.9-MeV transition, which has a rather peculiar looking angular distribution. No DWIA calculation was found that could fit this case well and the widest-angle points are fit best by a 6^- calculation. The problem with the points between 30° and 40° is probably due to fitting difficulties with the TOF spectra; however, refitting this region did not improve the results. In addition to 5^+ and 6^- stretched-state strengths, transitions are observed to three states, at 6.9, 7.0, and 8.2 MeV, which appear to carry 4^- strength.

The total 6^- $1\hbar\omega$ strength observed in the ^{24}Mg$(p,n)^{24}$Al reaction is summarized in Table I. The total strength observed is (62±10)% of the ESPHM expectation.

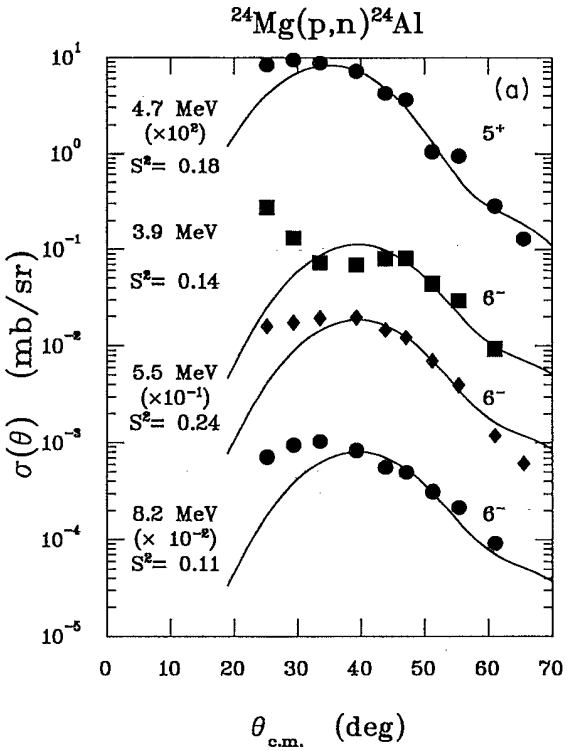

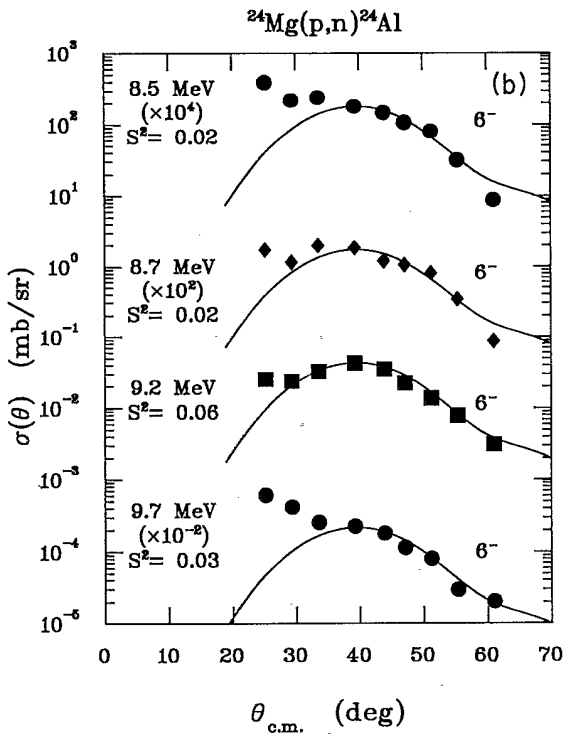

FIG. 8. Angular distributions for the 5^+ state at 4.7 MeV and the 6^- states at 3.9, 5.5, 8.2, 8.5, 8.7, 9.2, and 9.7 MeV in the ^{24}Mg$(p,n)^{24}$Al reaction at 136 MeV. The solid lines represent DWIA calculations (see the text).

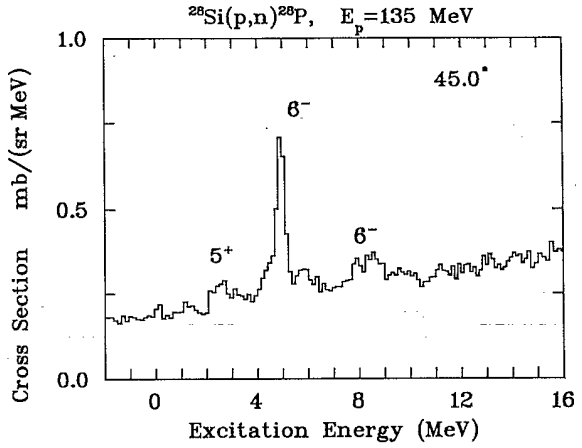

FIG. 9. Excitation-energy spectrum for the ^{28}Si$(p,n)^{28}$P reaction at 135 MeV and 45°.

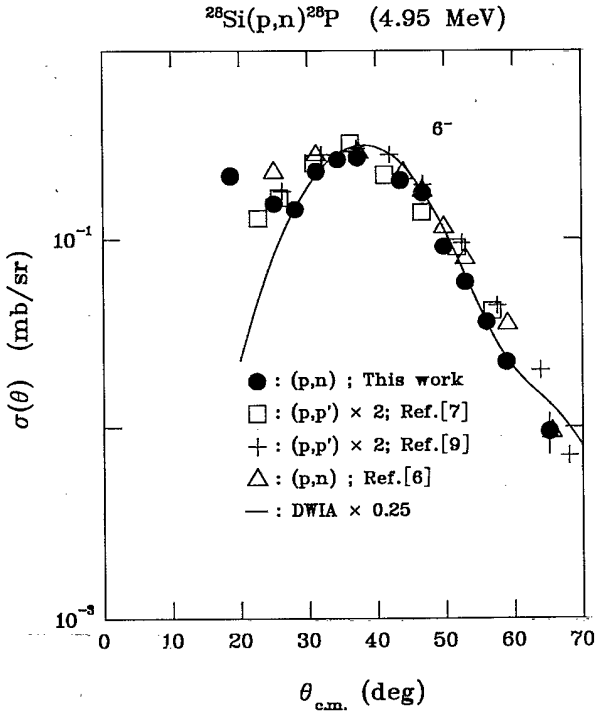

FIG. 10. Angular distribution for the 6^- state at 4.95 MeV in the ^{28}Si$(p,n)^{28}$P reaction at 135 MeV. Shown also for comparison are the results of an earlier (p,n) analysis and two (p,p') measurements to the analog 6^- state in ^{28}Si. The solid line represents a DWIA calculation (see the text).

C. The $^{28}Si(p,n)^{28}P$ reaction

The experimental excitation-energy plot for this reaction at 45° is shown in Fig. 9. The spectrum is dominated by the large 6^- peak at 4.95 MeV. This state is the analog of the known $T=1$, 6^- state at 14.35 MeV in ^{28}Si, which was studied in both inelastic electron and proton scattering, [7–9]. The (p,n) excitation of this state was reported earlier by Fazely *et al.* [6]. The angular distribution for this transition obtained in the present work is compared in Fig. 10 with the earlier (p,n) analysis and twice the (p,p') cross sections of Adams *et al.* [7] and Olmer *et al.* [9]. Although there is some scatter among these various results, they are in reasonably good agreement. Shown also are the results of a DWIA calculation for a $6^-,(f_{7/2},d_{5/2}^{-1})$ particle-hole excitation. The shapes of the experimental and DWIA angular distributions are in good agreement; the DWIA normalization factor required is 0.25, assuming the ESPHM.

In addition to the large 6^- state at 4.95 MeV, we see seven other states which appear to carry 6^- strength. The angular distributions for these transitions are compared in Fig. 11 with DWIA calculations for a 6^- transition. The summary of the 6^- strength observed in this reaction is presented in Table I. Besides the strong state at 4.95 MeV, the largest amount of 6^- strength is observed in a broad bump around 8 MeV (see Fig. 9). The DWIA fits to the angular distributions suggest that about 80% of this bump is 6^- strength (at 45°). The significant amount of 6^- strength seen about 3 MeV above the strong state at 4.95 MeV agrees with the recent, large-basis shell-model calculation of Carr [11]; this comparison will be discussed further in the next section. The total amount of 6^- strength observed is (43±7)% of that expected in the ESPHM.

Although one does not expect a $(d_{5/2},d_{5/2}^{-1}),5^+$ state in

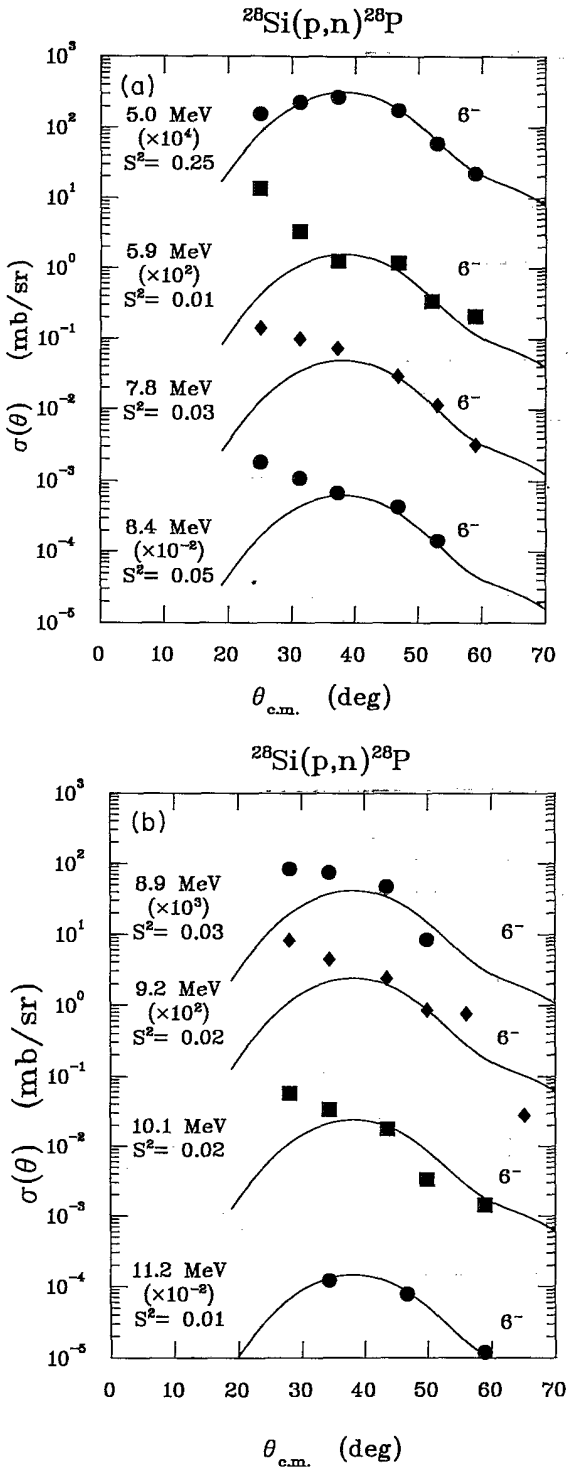

FIG. 11. Angular distributions for the 6^- states at 5.0, 5.9, 7.8, 8.4, 8.9, 9.2, 10.1, and 11.2 MeV in the $^{28}Si(p,n)^{28}P$ reaction at 135 MeV. The solid lines represent DWIA calculations (see the text).

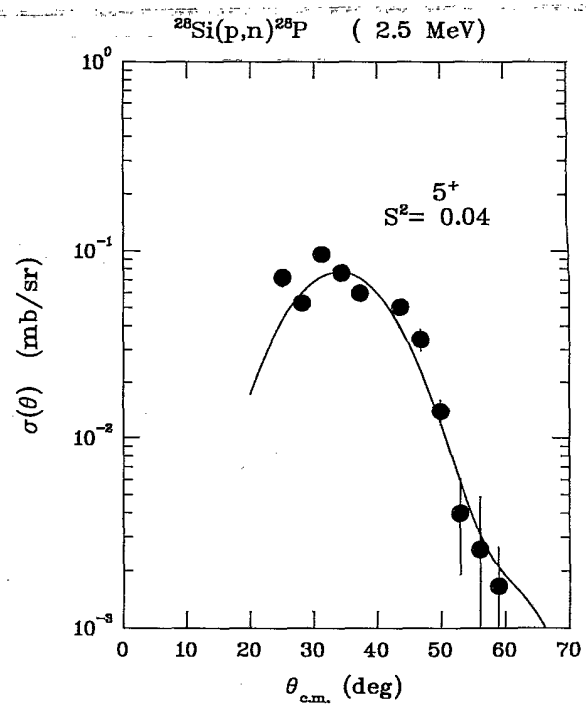

FIG. 12. Angular distribution for the 5^+ state at 2.54 MeV in the $^{28}Si(p,n)^{28}P$ reaction at 135 MeV. The solid line represents a DWIA calculation (see the text).

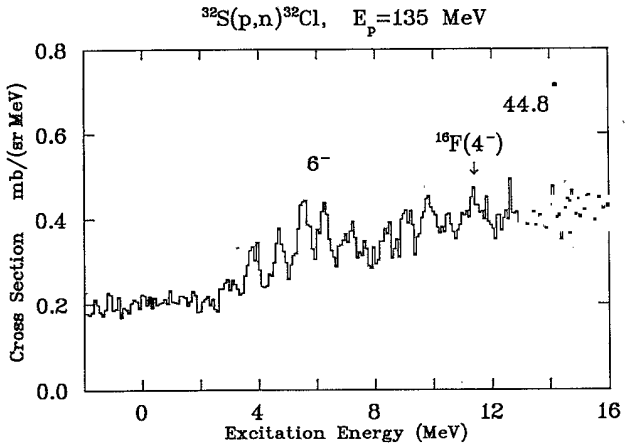

FIG. 13. Excitation-energy spectrum for the $^{32}S(p,n)^{32}Cl$ reaction at 135 MeV and 45°.

the $^{28}Si(p,n)$ reaction in the simple shell model, the state observed at 2.5 MeV appears to be such an excitation. The angular distribution for this transition is compared in Fig. 12 with a 5^+ DWIA calculation. The agreement between the measured and calculated angular distributions is excellent. The identification of this state as a 5^+ state is supported also by the fact that a 5^+ state is reported (tentatively) at 2.58 MeV in the $T=1$ analog nucleus ^{28}Al [26]. This excitation in the (p,n) reaction can proceed only if there are holes in the $d_{5/2}$ proton orbital. The DWIA normalization factor required corresponds to the strength expected if there is (on the average) about $\frac{1}{3}$ of a proton hole in the $d_{5/2}$ orbital. We see also a shoulder on the strong 6^- state at 4.95 MeV, which appears to have some 5^+ strength. We tentatively identify this state at 4.7 MeV with $\sim\frac{1}{3}$ the strength of the lower 5^+ state.

In addition to the 6^- and 5^+ strengths, 4^- strength is observed in five transitions to states at 3.2, 5.2, 7.8, 8.9, and 10.1 MeV. The summary of observed 6^- and 5^+ strengths is presented in Table I.

D. The $^{32}S(p,n)^{32}Cl$ reaction

The experimental excitation-energy plot for this reaction at 45° is shown in Fig. 13. The 6^- strength is highly fragmented and is observed in at least nine states between 3.8 and 9.8 MeV. This fragmentation was observed also for the analog $T=1$ states in ^{32}S in inelastic electron scattering, where nine states carrying 6^- strength are spread out over about 6 MeV of excitation [25]. No one state is clearly larger than all the others. This fragmentation is similar to that seen in the $^{40}Ca(p,n)^{40}Sc$ reaction [30], and is apparently due to the fragmentation of the $d_{5/2}$ orbital caused by the addition of nucleons in the $2s_{1/2}$ orbital.

The angular distributions for these nine 6^- states are shown in Fig. 14. The 6^- DWIA calculations are similar to those described earlier for the other targets, except that here the optical-model wave functions are calculated using the global optical-model parameter set of Schwandt *et al.* [31]. The calculation agrees well with the shape of the largest single state at 5.6 MeV. The summary of the 6^- strength observed in this reaction is presented in Table I. The total amount of the 6^- strength identified in

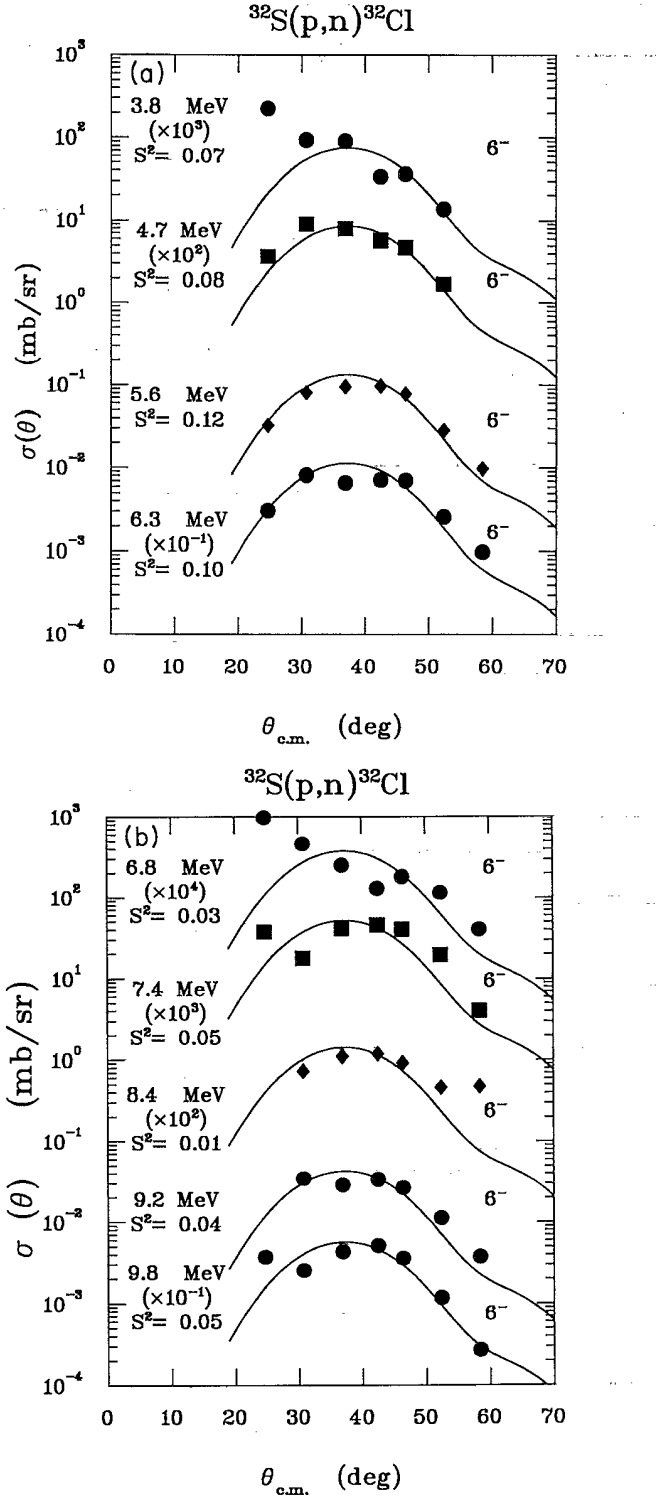

FIG. 14. Angular distributions for the 6^- states at 3.8, 4.7, 5.6, 6.3, 6.8, 7.4, 8.4, 9.2, and 9.8 MeV in the $^{32}S(p,n)^{32}Cl$ reaction at 135 MeV. The solid lines represent DWIA calculations (see the text).

these states is (55±9)% of that expected in the ESPHM. This amount is less than the 71% total observed in the inelastic-electron-scattering work. The difference is somewhat larger than the usual difference observed between (p,n) [and (p,p')] and (e,e') analysis of stretched-state strengths. A usual difference of about 20% is observed for several cases and may be due to certain meson-exchange contributions not included in the (e,e') reaction calculations, and which are not significant in the (p,n) reaction [1].

V. COMPARISONS WITH SHELL-MODEL CALCULATIONS

In this section, we compare the experimental results described above with shell-model calculations performed to try to predict the 5^+ and 6^- distributions in these (p,n) reactions. These comparisons are made separately for the 5^+ and 6^- excitations as described below.

A. The 5^+ $0\hbar\omega$ excitations

The shell-model calculations for the $(d_{5/2},d_{5/2}^{-1})$, 5^+ excitations were all performed with the computer code OXBASH [27]. These calculations were all unrestricted in the *s-d* shell, i.e., they assumed that the number of particles that one would predict to be in the *s-d* shell with a closed ^{16}O core could be arranged without restriction in the *s-d* shell-model orbitals (satisfying isospin requirements). These calculations provide 21, 325, 839, and 325 0^+ states, respectively, for ^{20}Ne, ^{24}Mg, ^{28}Si, and ^{32}S, and 34, 1791, 5755, and 1791 5^+ states, respectively, for ^{20}Na, ^{24}Al, ^{28}P, and ^{32}Cl. The interaction used in these calculations is the "universal" *s-d* interaction of Wildenthal [28]. This basis and interaction are known to describe energy levels and other observables in the *s-d* shell remarkably well [28]. This basis and interaction were used also to describe the 1^+, "Gamow-Teller" (GT) strength distributions in these same (p,n) reactions [32,16]. The ^{24}Mg$(p,n)^{24}$Al and ^{32}S$(p,n)^{32}$Cl GT distributions were described well by these calculations; but the ^{20}Ne$(p,n)^{20}$Na and ^{28}Si$(p,n)^{28}$P GT distributions were not. The poor agreement for the former is likely because the assumption of a closed ^{16}O core for ^{20}Ne is probably

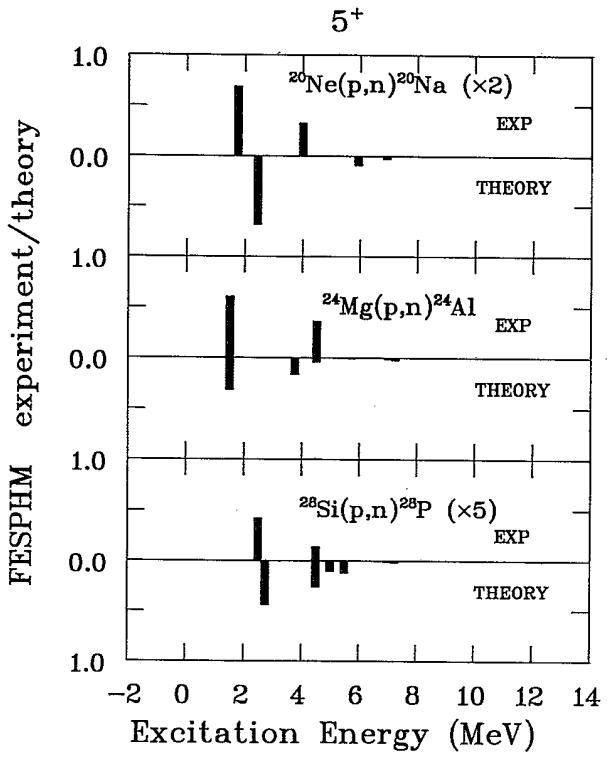

FIG. 15. Comparison of the experimental and theoretical 5^+ distributions for the ^{20}Ne, ^{24}Mg, and ^{28}Si(p,n) reactions (see the text).

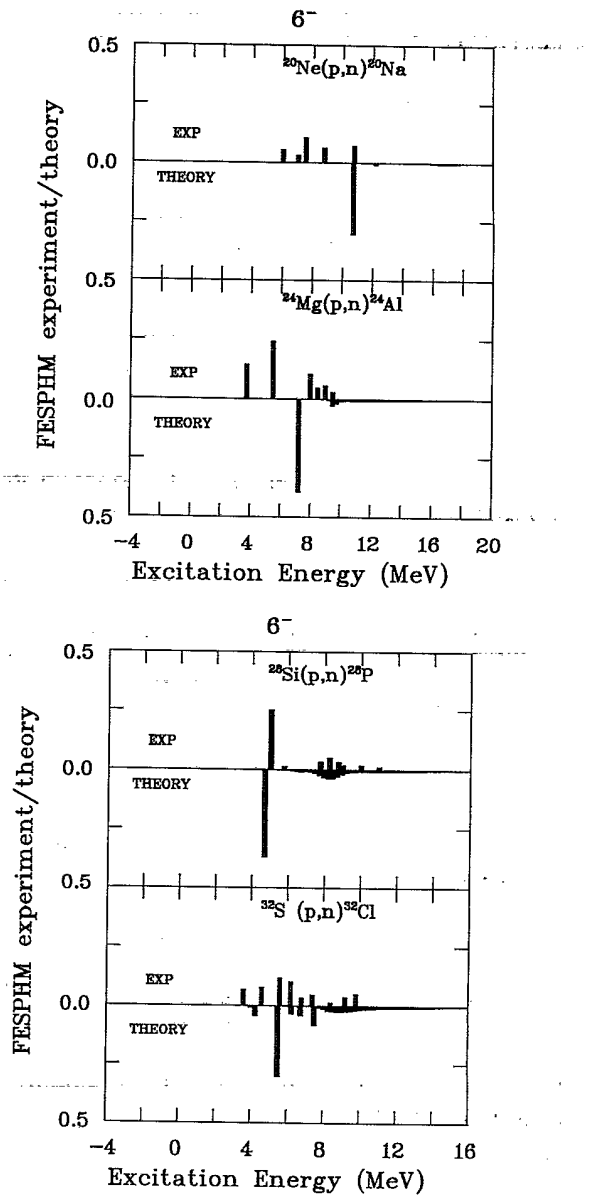

FIG. 16. Comparison of the experimental and theoretical 6^- distributions for the ^{20}Ne, ^{24}Mg, ^{28}Si, and ^{32}S(p,n) reactions (see the text).

not valid; the poor agreement observed for the latter case is more puzzling, since ^{28}Si is at the middle of the *s-d* shell and might be expected to be described well by such calculations.

The comparisons for the 5^+ excitations are shown in Fig. 15. No 5^+ excitations are observed in the ^{32}S$(p,n)^{32}$Cl reaction and none are predicted with measurable strength. For the ^{20}Ne, ^{24}Mg, and ^{28}Si(p,n) reactions, the excitation energy of the lowest (and largest) 5^+ excitations are all predicted well. For all three of these reactions, additional weaker 5^+ strength is predicted and observed a few MeV above the lowest state. In this sense, the shell-model calculations appear relatively successful; it should be noted, however, that in all three reactions, the observed 5^+ strength is actually somewhat *greater* than that predicted by the calculations.

B. The 6^- $1\hbar\omega$ excitations

The shell-model calculations for the $(f_{7/2},d_{5/2}^{-1}),6^-$ excitations were all performed with the VLADIMIR system of codes [11,33], adapted to the ETA10 and Cray YMP computers at the Florida State University Supercomputer Computations Research Institute. For all of these calculations [34], the 0^+ target wave functions were restricted to the *s-d* shell. The 6^- final-state wave functions required one particle to be in the $f_{7/2}$ orbital with the remainder unrestricted in the *s-d* shell.

The comparisons for the 6^- excitations are shown in Fig. 16. For the ^{20}Ne and ^{24}Mg(p,n) reactions, we see that while the shell-model calculations predict roughly the correct centroid of the observed 6^- strength, the calculations predict basically only one strong state, while experimentally the strength is highly fragmented. The total 6^- strength predicted in these two reactions is somewhat greater than that observed.

For the ^{28}Si and ^{32}S(p,n) reactions, the shell-model calculations describe the experimental distributions remarkably well. For the ^{28}Si$(p,n)^{28}$P reaction, the 6^- state at 4.95 MeV clearly dominates the spectrum, with some additional 6^- strength observed about 3 MeV higher. These results are described well by the large-basis shell-model calculations. For the ^{32}S$(p,n)^{32}$Cl reaction, the 6^- strength is observed to be highly fragmented, with no one state dominating the spectrum. Although the shell-model calculations do not perfectly reproduce the observed fragmentation, the general amount and overall width of this fragmentation is clearly described well. We note here that the observed 6^- distributions in ^{28}P and ^{32}Cl are also in good agreement with the analog 6^- strength distributions observed in inelastic electron scattering. The good success of these shell-model calculations in describing these distributions indicates that realistic, large-basis shell-model calculations can reasonably describe both the distribution and total strength of these simple particle-hole states.

Regarding the comparison of the total strength predicted by these calculations with that observed, we see 53, 83, 56, and 61% of the strength predicted by the large-basis calculations [34] for ^{20}Ne, ^{24}Mg, ^{28}Si, and ^{32}S(p,n), respectively. Thus, we see about $\frac{2}{3}$ of that predicted. Some of the difference is certainly in small states in the continuum, that are too difficult to see experimentally.

VI. CONCLUSIONS

Both 5^+ $0\hbar\omega$ and 6^- $1\hbar\omega$ stretched-state strength is observed in the (p,n) reaction on all the self-conjugate, *s-d* shell, targets ^{20}Ne, ^{24}Mg, and ^{28}Si. For the (p,n) reaction on ^{32}S, 6^- strength only is observed.

In the ^{20}Ne(p,n) and ^{24}Mg(p,n) reactions, the majority of the $(d_{5/2},d_{5/2}^{-1})$, 5^+ $0\hbar\omega$ strength is observed in single states at low excitation energy that have strengths consistent with that calculated in the DWIA using full *s-d* shell-model wave functions. A small amount of 5^+ strength is seen also in both reactions at somewhat higher excitation energies. These observations agree with the shell-model predictions.

A weak 5^+ state is observed in the ^{28}Si$(p,n)^{28}$P reaction at 2.5 MeV. The excitation energy of this state agrees well with the excitation energy of a tentatively reported 5^+ state in the analog nucleus ^{28}Al. This excitation can occur only if there are holes in the $d_{5/2}$ proton orbital and the strength observed corresponds to about $\frac{1}{3}$ of a proton hole. A second, smaller 5^+ state may be observed at 4.7 MeV. These experimental results are reproduced well by a full *s-d* basis shell-model calculation.

The $(f_{7/2},d_{5/2}^{-1})6^-$ $1\hbar\omega$ strength is fragmented in all four reactions. The analog of the strongest single transition in the $A=24$ and 28 systems have been observed in ^{24}Mg and ^{28}Si in inelastic electron and proton scattering; the (p,n) angular distributions for these transitions are in good agreement with these analog transitions. Because the (p,n) reaction suppresses the isoscalar ($T=0$) background, the isovector ($T=1$) 6^- strength can be identified, even though it is fragmented. In the ^{20}Ne$(p,n)^{20}$Na reaction, 6^- strength is identified in five states which carry 32% of the extreme single-particle-hole strength (ESPHM) expected in the simple shell model. In the ^{24}Mg$(p,n)^{24}$Al reaction, 6^- strength is identified in seven states, which carry 62% of the ESPHM strength. In the ^{28}Si$(p,n)^{28}$P reaction, 6^- strength is observed in eight states, which carry 43% of the ESPHM strength. In the ^{32}S$(p,n)^{32}$C reaction, 6^- strength is observed in nine states, which carry a total of 55% of the ESPHM. For each of the first three reactions, a single state dominates the spectrum. For the ^{32}S$(p,n)^{32}$Cl reaction, the 6^- strength is spread out over about 7 MeV with no single state dominant.

Large-basis shell-model calculations [34] were compared with these observed 6^- strength distributions. These calculations allow for unrestricted excitations in the *s-d* shell, coupled to the $(f_{7/2},d_{5/2}^{-1})$ configuration for the final state. The calculations reproduce the ^{28}Si$(p,n)^{28}$P spectrum remarkably well, even reproducing the small amount of 6^- strength observed about 3 MeV above the large state at 4.95 MeV. These calculations also generally reproduce the large 6^- fragmentation observed in the ^{32}S$(p,n)^{32}$Cl reaction. These calculations do not reproduce the ^{20}Ne and ^{24}Mg(p,n) 6^- distributions as well; the observed spectra are fragmented while

the predicted spectra show essentially only one strong state in each case. It may be that the fragmentation of the 6^- strength in the $A=20$ and 24 systems is due mainly to the fragmentation of the high-lying $f_{7/2}$ orbital, whereas for the $A=28$ and 32 systems it is due to the fragmentation of the $d_{5/2}$ orbital as it is pushed down below the Fermi surface. The calculations presented here allow for multiparticle-multihole excitations in the *s-d* shell and may be able to reproduce the latter but not the former. It is also the case that the *sd-f* Hamiltonian used in the calculations was not A dependent and is probably too weak for the lighter-mass nuclei considered here.

ACKNOWLEDGMENTS

This work was supported in part by the National Science Foundation and by the Department of Energy, Contract No. DE-FCO5-84ER250000.

[1] R. A. Lindgren, M. Leuschner, B. L. Clausen, R. J. Peterson, M. A. Plum, and F. Petrovich, in *Nuclear Structure at High Spin, Excitation, and Momentum Transfer* (McCormick's Creek State Park, Bloomington, Indiana), Proceedings of the Workshop on Nuclear Structure at High Spin, Excitation and Momentum Transfer, edited by H. Nann, AIP Conf. Proc. No. 142 (AIP, New York, 1986), p. 133.

[2] R. J. Peterson, B. L. Clausen, J. J. Kraushaar, H. Nann, W. W. Jacobs, R. A. Lindgren, and M. A. Plum, Phys. Rev. C **33**, 31 (1986).

[3] B. D. Anderson, J. W. Watson, and R. Madey, in *Nuclear Structure at High Spin, Excitation, and Momentum Transfer* [1], p. 155.

[4] B. D. Anderson, A. Fazely, R. J. McCarthy, P. C. Tandy, J. W. Watson, R. Madey, W. Bertozzi, T. N. Buti, J. M. Finn, J. Kelly, M. A. Kovash, B. Pugh, B. H Wildenthal, and C. C. Foster, Phys. Rev. C **27**, 1387 (1983).

[5] T. Chittrakarn, B. D. Anderson, A. R. Baldwin, C. Lebo, R. Madey, J. W. Watson, and C. C. Foster, Phys. Rev. C **34**, 80 (1986).

[6] A. Fazely, R. Madey, B. D. Anderson, A. R. Baldwin, C. Lebo, P. C. Tandy, J. W. Watson, W. Bertozzi, T. Buti, M. Finn, C. Hyde-Wright, J. Kelly, M. A. Kovash, B. Murdock, B. Pugh, and C. C. Foster, Nucl. Phys. **A443**, 29 (1985).

[7] G. S. Adams, A. D. Bacher, G. T. Emery, W. P. Jones, R. T. Konzes, D. W. Miller, A. Picklesimer, and G. E. Walker, Phys. Rev. Lett. **38**, 1387 (1977).

[8] C. Olmer, A. D. Bacher, G. T. Emery, W. P. Jones, D. W. Miller, H. Nann, P. Schwandt, S. Yen, T. E. Drake, and R. J. Sobie, Phys. Rev. C **29**, 361 (1984).

[9] H. Zarek, B. O. Pich, T. E. Drake, D. J. Rowe, W. Bertozzi, C. Creswell, A. Hirsch, M. V. Hynes, S. Kowalski, B. Norum, F. N. Rad, C. P. Sargent, C. F. Williamson, and R. A. Lindgren, Phys. Rev. Lett. **38**, 750 (1977).

[10] A. Amusa and R. D. Lawson, Phys. Rev. Lett. **51**, 103 (1983).

[11] J. A. Carr, S. D. Bloom, F. Petrovich, and R. J. Philpott, Phys. Rev. Lett. **62**, 2249 (1989).

[12] B. D. Anderson, C. Lebo, A. R. Baldwin, T. Chittrakarn, R. Madey, J. W. Watson, and C. C. Foster, Phys. Rev. Lett. **52**, 1872 (1984).

[13] N. Tamimi, Ph.D. dissertation, Kent State University, 1989 (unpublished).

[14] B. D. Anderson, T. Chittrakarn, A. R. Baldwin, C. Lebo, R. Madey, R. J. McCarthy, J. W. Watson, B. A. Brown, and C. C. Foster, Phys. Rev. C **31**, 1147 (1985).

[15] R. Madey *et al.*, Nucl. Instrum. Methods **214**, 401 (1983).

[16] B. D. Anderson, T. Chittrakarn, A. R. Baldwin, C. Lebo, R. Madey, P. C. Tandy, J. W. Watson, C. C. Foster, B. A. Brown, and B. H. Wildenthal, Phys. Rev. C **36**, 2195 (1987).

[17] P. R. Bevington, *Data Reduction and Error Analysis for the Physical Sciences* (McGraw-Hill, New York, 1969), p. 237.

[18] R. Cecil, B. D. Anderson, and R. Madey, Nucl. Instrum. Methods **161**, 439 (1979).

[19] J. W. Watson, B. D. Anderson, A. R. Baldwin, C. Lebo, B. Flanders, W. Pairsuwan, R. Madey, and C. C. Foster, Nucl. Instrum. Methods **215**, 413 (1983).

[20] J. D'Auria, M. Dombsky, L. Moritz, T. Ruth, G. Sheffer, T. E. Ward, C. C. Foster, J. W. Watson, B. D. Anderson, and J. Rapaport, Phys. Rev. C **30**, 1999 (1984).

[21] R. Schaeffer and J. Raynal, program DWBA70 (unpublished); J. R. Comfort, extended version DW81 (unpublished).

[22] M. A. Franey and W. G. Love, Phys. Rev. C **31**, 488 (1985).

[23] J. R. Comfort, G. L. Moake, C. C. Foster, P. Schwandt, C. D. Goodman, J. Rapaport, and W. G. Love, Phys. Rev. C **24**, 1834 (1981); R. A. Lindgren, J. Phys. (Paris) Colloq. **45**, C4-433 (1984).

[24] J. Blomquist and A. Molinari, Nucl. Phys. **A106**, 545 (1968).

[25] B. L. Clausen, R. A. Lindgren, M. Farkhondeh, L. W. Fagg, D. I. Sober, C. W. de Jager, H. de Vries, N. Kalantar-Nayestanaki, B. L. Berman, K. S. Dhuga, J. A. Carr, F. Petrovich, and P. E. Burt, Phys. Rev. Lett. **65**, 547 (1990).

[26] C. M. Lederer and V. S. Shirley, *Table of Isotopes* (Wiley, New York, 1978).

[27] B. A. Brown, A. Etchegoyen, W. D. M. Rae, and N. S. Godwin, program OXBASH (unpublished).

[28] B. H. Wildenthal, Prog. Part. Nucl. Phys. **11**, 5 (1984).

[29] D. J. Millener and D. Kurath, Nucl. Phys. **A255**, 315 (1975).

[30] B. D. Anderson, J. W. Watson, C. Lebo, A. R. Baldwin, A. Fazely, R. Madey, and C. C. Foster, Phys. Lett. **123B**, 383 (1983).

[31] P. Schwandt, H. O. Meyer, W. W. Jacobs, A. D. Bacher, S. E. Vigdor, M. D. Kaitchuck, and T. R. Donoghue, Phys. Rev. C **26**, 55 (1982).

[32] B. D. Anderson, N. Tamimi, A. R. Baldwin, M. Elaasar, R. Madey, D. M. Manley, M. Mostajabodda'vati, J. W. Watson, W. M. Zhang, and C. C. Foster, Phys. Rev. C **43**, 50 (1991).

[33] R. F. Hausman, LLNL Report No. UCRL-52178, 1976 (unpublished).

[34] J. A. Carr, S. D. Bloom, F. Petrovich, and R. J. Philpott, Phys. Rev. C **45**, 1145 (1992), this issue.